Dalton Transactions

Accepted Manuscript

ROYAL SOCIETY OF CHEMISTRY

www.rsc.org/dalton

Cite this: DOI: 10.1039/c0xx00000x

www.rsc.org/xxxxxx

ARTICLE TYPE

Manganese-Mefenamic Acid Complexes Exhibit High Lipoxygenase Inhibitory Activity

Jie Feng, Xin Du, Hui Liu, Xin Sui, Chen Zhang, Yun Tang, Jingyan Zhang

State Key Laboratory of Bioreactor Engineering, Shanghai Key Laboratory of New Drug Design, School of Pharmacy, East China University of Science and Technology, Shanghai, 200237. P. R. China. Email: jyzhang@ecust.edu.cn, Fax/Tel:0086-021-64253846

Received (in XXX, XXX) Xth XXXXXXXXX 20XX, Accepted Xth XXXXXXXXX 20XX
DOI: 10.1039/b000000x

The coordination of non-steroidal anti-inflammatory drugs (NSAIDs) to metal ions could improve the pharmaceutical efficacy of NSAIDs due to the unique characteristics of metal complexes. However, the structures of many metal-NSAID complexes are not well characterized, the functional mechanism and pharmaceutical effect of these complexes thus are not fully understood. In this work, three manganese-mefenamic acid (Mn-mef) complexes were synthesized and structurally characterized, and their pharmaceutical effect was investigated. We found that the three Mn-mef complexes exhibit higher lipoxygenase (LOX-1) inhibitory activity (IC_{50} are 16.79, 38.63 and 28.06 μM, respectively) than that of the parent ligand mefenamic acid (78.67μM). More importantly, the high inhibitory activity of the Mn-mef complexes is closely related to their spatial arrangements, which determine their interaction with LOX-1. Computer docking of the Mn-mef complexes with the LOX-1 confirms the experimental results: smaller Mn-mef complexes tend to bind competitively to LOX-1 at the substrate binding site, which is also analogous to the binding of ligand mefenamic acid; while the bulky metal complexes inhibit the enzyme activity un-competitively. In addition, the Mn-mef complexes display higher anti-oxidant activity than that of ligand mefenamic acid. The higher anti-oxidant activity of the Mn-mef complexes apparently originated from the manganese centre of the complexes. We thus conclude that Mn-mef complexes enhance the anti-inflammatory activity of mefenamic acid by increasing their activity *via* changing their interaction mode with the enzymes, and/or improving their anti-oxidant ability using metal ion. This work provides experimental evidence that with the unique spatial arrangements, metal-NSAID complexes could interact with the target enzymes more specifically and efficiently, which is superior to their ligand NSAIDs.

Introduction

Non-steroidal anti-inflammatory drugs (NSAIDs) that employed to alleviate inflammation and pain associated with diseases exert their therapeutic effects by inhibiting prostaglandins and thromboxanes synthesis, which were derived from the enzymatic transformation of arachidonic acid by cyclooxygenase (COX) and lipoxygenase (LOX) enzymes, respectively.[1-4] However, NSAID-induced side effects, particularly in the gastrointestinal tract and the kidney, are often limited their applications.[5-6] For that reason, considerable efforts have been made to increase their potencies while minimize their side effects. Chemical modification of the structure of NSAIDs is often used strategy to improve the performance of NSAIDs.[7-8] While the coordination of NSAIDs to metal ions is one of the fast developing directions because the divalent metal ions may impose extra properties to the NSAIDs ligands.[9] In comparison to NSAIDs, metal-NSAID complexes have many more coordination numbers, geometries, and oxidation/reduction states that can be used to make structures that interact with targets in unique ways. These are unavailable to most NSAIDs. Numerous metal complexes with NSAIDs as ligands have been shown more potent than either the parent NSAID drugs or the un-complexed metal salts. For example, Regtop *et al.* found that copper and zinc complexes of indomethacin could improve the pharmacological profiles of indomethacin and reduce their toxicity.[10] Konstandinidou et al. reported the anti-inflammatory activity of diclofenac could be enhanced by the coordination with Co^{2+}, Ni^{2+}, and Pd^{2+} ions, because these metal complexes could offer significant protection

against lipid peroxidation *in vitro*.[11] Some Cu-NSAID complexes also exhibit potent SOD or anti-inflammatory activity.[9, 12] However, the structures of the metal-NSAID complexes in most cases are not well characterized, some of them are just the mixtures of the metal ions and NSAIDs, hence the improvement of the anti-inflammatory activity of NSAIDs by the coordination to metal ions is still need to be studied.

Mefenamic acid (2-(2,3-dimethylphenyl) amino benzoic acid, mef) is one of the most effective NSAIDs that used in clinic, which exhibited favourable anti-inflammatory, analgesic properties, but it exhibits side effects as other NSAIDs.[13] Kovala-Demertzi *et al.* tempted to improve its activity and decrease its side effect by preparing different metal-mef complexes, including Cu^{2+}, Zn^{2+}, Mn^{2+}, Co^{2+}, and Ni^{2+} complexes. Their biological responses in terms of antioxidant activity, LOX inhibition, and trypsin induced proteolysis were compared; the anti-proliferative activity and anti-inflammatory activity of some compounds were also investigated.[14] Later, Psomas *et al.* from the same university also reported Co-mef and Cu-mef complexes.[15-16] In that work, they focused more on the interaction of these complexes with DNA and bovine serum albumin in addition to the anti-oxidant and LOX inhibitory activities. Spectroscopic analysis and the pharmacology activity of Sn-mef complex were also reported,[17] but tin itself is a toxic element exerting profound adverse effects on many life processes.[18] Though excess manganese in brain may also induce permanent neurodegenerative damage, resulting in a syndrome similar to Parkinson's disease,[19] manganese is an essential trace element for human being and a cofactor for a number of enzymes.[20] Many metal-mef complexes have been reported so far, most of them are not structurally defined, their biological response and pharmaceutical properties could not be correlated well with their structures, or tuned according to their structures.

In this study, three Mn-mef complexes, $Mn(mef)_2(CH_3OH)_4$ (**1**), $Mn(mef)_2(bipy)(CH_3OH)_2$ (**2**), and $Mn(mef)_2(phen)H_2O$ (**3**), (bipy = 2, 2′-bipyridyl, phen = phenathroline), were structurally well characterized, their LOX-1 inhibitory activity and antioxidant ability were examined experimentally in parallel with the parent drug mefenamic acid. The binding of the three complexes to the LOX-1 was investigated *via in silico* docking as well. The results clearly indicated that Mn-mef complexes exhibit high LOX-1 inhibitory activity than mefenamic acid, which can be attributed to the different interaction modes of the Mn-mef complexes with LOX-1. Manganese is an essential trace element, and is a less toxic element,[21] Mn-mef complexes hence show great promise as pharmaceutical reagents.

Experimental section

Materials and methods

All reagents and organic solvents were analytical grade and used as received without further purification. 1,1-diphenyl-2-picrylhydrazyl (DPPH) was purchased from Alfa Aesar Company, and lipoxygenase (EC 1.13.11.12, LOX-1) was obtained from Sigma-Aldrich Company, the others were from SinoPharm Chemical Reagent Co., Ltd. Superoxide dismutase (SOD) assay kit was purchased from Jiancheng Bioengineering Institute (Nanjing, China). Electronic absorption spectra were recorded on a Cary 50 spectrophotometer with quartz cuvettes (Varian, USA). Elemental analyses of the all complexes were performed with an elementar vario EL III analyzer (Germany). X-Band EPR spectra were acquired on EMS spectrometer (Bruker, USA) with a cryostat ESR-900 system (Oxford, UK). Conductivity measurements were carried out with HI8733 conductivity meter using methanol as a solvent. X-ray crystallographic data of the complexes was collected on a SMART diffractometer (Bruker, USA) using Mo-Kα radiation (λ = 0.71 Å). The structure was solved by direct methods (SHELXS-97) and refined with full-matrixleast-square techniques on F^2 using SHELXL-97. Mass Spectrometry data were acquired by LCQ Deca XP Plus Quadrupole Ion Trap Mass Spectrometer (Thermo Finnigan, USA)

Preparation of Mn-mef complexes

$Mn(mef)_2(CH_3OH)_4$ (1). Mefenamic acid (0.4 mmol, 96.4 mg) and KOH (0.4 mmol, 22.4 mg) were added to 15 mL of methanolic solution and stirred for 1 h. The solution was then added to a methanolic solution (10 mL) of $MnCl_2{\cdot}4H_2O$ (0.2 mmol, 39.5 mg). The reaction mixture was stirred for 2 h at room temperature. The resulting solution was filtered, light-yellow block crystals that suitable for X-ray structure analysis were obtained by slow evaporation of the filtrate, collected by filtration, washed with diethyl ether and dried in air. Yield: 53.75% (based on the manganese salts). Elemental analysis data: calculated. (%) for $C_{34}H_{44}MnN_2O_8$ (Mw 663.25): C, 61.53; H, 6.68; N, 4.22. Found (%): C, 61.28; H, 6.54; N, 4.22.

$Mn(mef)_2(bipy)(CH_3OH)_2$ (2). A methanolic solution (15 mL) of mefenamic acid (0.4 mmol, 96.4 mg) and KOH (0.4 mmol, 22.4 mg) was stirred for 1 h. This solution was then mixed with a methanolic solution of 2, 2'-bipyridyl (0.2 mmol, 31.2 mg) and a methanolic solution (10 mL) of $MnCl_2{\cdot}4H_2O$ (0.2 mmol, 39.5 mg). The obtained solution was stirred for 2 h and filtered. Light-yellow well-shaped crystals that were suitable for X-ray diffraction were obtained after three weeks. The crystals were collected by filtration, washed with diethyl ether and dried in air. Yield: 67.55% (based on the manganese salts). Elemental analysis data: calculated. (%) for $C_{42}H_{44}MnN_4O_6$ (Mw 755.75): C, 66.75; H, 5.87; N, 7.41. Found (%): C, 66.43; H, 5.53; N, 7.54.

$Mn(mef)_2(phen)H_2O$ (3). The complex **3** were obtained with the same procedure used for the complex 2 but using phenanthroline (0.2 mmol, 39.6 mg) instead of 2,2'-bipyridyl. The reaction mixture was filtered and washed by water. Then the filtration was dissolved in DMF for slow evaporation. The microcrystalline product was collected after a few days, washed by a slight of methanol and dried in air, which is just suitable for X-ray diffraction. Yield: ca. 48%. Elemental analysis data: calculated. (%) for $C_{42}H_{38}MnN_4O_5$ (Mw 733.70): C, 68.75; H, 5.22; N, 7.64. Found (%): C, 69.07; H, 5.39; N, 7.49.

The corresponding three Co-mef complexes were synthesized and characterized according to the literature.[15]

Mass spectrometry

All mass spectra were collected on a Quadrupole Ion Trap Mass Spectrometer (Thermo Finnigan, USA) fitted with an electrospray interface and operated in the positive inonization mode. Samples were all dissolved in DMF and applied *via* a direct infusion method at a flow rate of 3 μL/min. The analysis was performed

using the following parameters: spray voltage, 4.8 kV; capillary temperature, 275 ℃; capillary voltage, 15 V. And nitrogen was used as the nebulizer gas.

LOX-1 inhibition

LOX-1 (10^{-6} mM) was added to borate buffer (0.1 M, pH 9.0) containing different concentrations of the complexes (complex **1**, **2** or **3**). The reaction was initiated by adding the substrate linoleic acid (0.75 mM), and the absorbance at 235 nm was measured after 5 min of the reaction in dark. The inhibition of the complexes was determined by the equation: Lipoxygenase activity (%) = $(A'/A_0)\times100$, where A′ is absorbance of reaction with the complex, A_0 is absorbance of reaction without the complex, respectively.[22]

Computer docking

The docking experiments were performed using the free trial of Molegro Virtual Docker software (MVD; version-6.0) obtained from the homepage of Molegro (http://www.clcbio.com/products/molegro-virtual-docker/#trial). The crystal structure of LOX-1 was download from the PDB protein data bank (PDB ID: 1F8N). The crystal structures of the complex were converted as MOL format using Diamond software. The water molecules in LOX-1 were removed and explicit hydrogen atoms were added to the complexes during the preparation by MVD. The docking of the complexes with LOX-1 was performed at the vicinity of the active site of LOX-1 based on the previously published crystal structure of LOX-1.[23] A sphere of a radius of 25 Å that centring at the Fe atom (coordination in the LOX-1: 24.53, 44.38, 10.60) of the LOX-1, covering the whole active site of LOX-1 and almost the whole C-domain, was employed as the docking area in the LOX-1. Docking calculations were carried out using the heustic search algorithm MolDock SE (simplex evolution), which was used as a search algorithm in combination with the grid-based version of the MolDock Scores [GRID] in the analysis.[24] Once the complex and LOX-1 were imported to the program, structural parameters including bond type, hybridization, explicit hydrogen atoms, charges, and flexible torsions were assigned using the automatic preparation function in MVD software. The grid resolution was set to 0.30 Å, the maximum population size and interactions were set to 50 and 1500, respectively. In the ligand map, the hydrogen bonding and steric minimum strength were set to 0.625. Ten independent runs were carried out for each docking. During the docking, the complexes were treated as flexible molecules, whereas the LOX-1 was regarded rigid.[24] The best docking results were selected on the basis of MolDock Score, Rerank Score and hydrogen bond.[25]

Anti-oxidant activity

The solutions were prepared as the following: 0.5 mL methanolic solution of the complex (0.2 mM) was mixed with DPPH methanolic solution (60 μM, 0.5 mL) in the dark. The samples were incubated at 25℃ for 30 min in the dark to reach the equilibrium before the measurement. The radical scavenging ability (I) of the three complexes were calculated using the equation: $I\% = (1- A_s/A_0) \times 100$, where A_0 is absorbance of the sample at 0 min and A_S is the absorbance of the sample at 30 minute, respectively.

A commercial superoxidase (SOD) kit was used to measure the $O_2^{\cdot -}$ scavenging ability of the complexes **1-3** and mefenamic acid. $O_2^{\cdot -}$ was generated by xanthine-xanthine oxidase through oxidizing hydroxylamine to nitrite, which has a sharp absorbance at 550 nm after the reaction with the color-developing agent. The percentage of SOD activity inhibitory is calculated according to the equation: SOD activity inhibitory (%)=$(A_{balnk}-A_{sample})/A_{blank}\times100$.

Results and discussion

Structures of the Mn-mef complexes

The structures of the complexes **1-3** were determined by single crystal X-ray diffraction (Detailed crystallographic data and the structures are given in Table 1 and Fig. 1, respectively). Selected bond lengths and angles of the complexes are summarized in Tables 2. As shown in Fig. 1, complex **1** is a centrosymmetric mononuclear manganese complex with two mef ligands and four methanol molecules. There are two methanol molecules are in the unit cell of the crystal of complex **1**. The manganese centre is in a six coordinated octahedral geometry. The four equatorial sites are occupied by two oxygen atoms of methanol (Mn1-O4(4′), 2.213(3) Å) and two oxygen atoms from the two monodentate mef ligands (Mn1-O1(1′), 2.129(19) Å). The apical positions are occupied by two oxygen atoms of methanol with Mn1-O3(3′) bond length of 2.202(2) Å. Apparently, the Mn-O bonds formed with mef are stronger than that with methanol molecules. The Mn atom lies below the basal plane by 0.0221 Å. Complex **1** is structurally similar to $Co(mef)_2(MeOH)_4$, except slight longer Mn-O distance than Co-O ($Co\text{-}O_{carboxylic}$ 2.062(2) Å, $Co\text{-}O_{metholic}$ 2.084(3), 2.063(3) Å).[15]

Comparing to the complex **1**, the manganese centre in complex **2** is in a distorted octahedral geometry with a N_2O_4 ligand set composed by two O atoms from two mef ligands, two O atoms of methanol, and two N atoms from 2, 2'-bipyridyl, which is very similar to cobalt complexes with the same ligands.[15] There are no methanol in copper complex $[Cu(mef)_2(bipy)]$, instead, the copper atom is six-coordinate and is surrounded by two mef ligands and a bidentate 2, 2'-bipyridyl ligand showing a distorted octahedral geometry.[15] In the complex **2**, O3, O3′, N2, and N2′ define a basal plane centred with Mn atom. The $Mn\text{-}N_{bipy}$ bond distance (2.232(4) Å) is in a good agreement with the same bond reported in the literature,[26] but is longer than $Co\text{-}N_{bipy}$ (2.115(3) Å) and $Cu\text{-}N_{bipy}$ (1.997(2), 2.006(2) Å).[15-16] The $Mn\text{-}O_{metholic}$ bond distance is 2.141(4) Å, which is slight shorter than that in the complex **1**, while the $Mn\text{-}O_{carboxylic}$ bond distance of 2.126(2) Å is comparable to those in the complex **1**. Similar to the complex **1**, manganese complex **2** has a longer Mn-O bond than cobalt complexes and copper complexes.[15-16] The methanol molecules are lying at cis positions (O(3)-Mn(1)-O(3′) = 96.8(3)°) and the oxygen atoms from mefenamic acid are in trans position (O(1)-Mn(1)-O(1′) = 177.4(2)), which is more distorted than that in $Co(mef)_2(bipy)(MeOH)_2$.[15]

The complex **2** is not symmetric, although two oxygen atoms from methanol, two nitrogen and two oxygen atoms from ligand mef are coordinated equally to manganese atom. The two mef ligands are orientated in the same direction on the two sides of the Mn-bipy plane, while in the complex **1**, two mef ligands are

central symmetric around the manganese centre. The overall structural difference between the complexes **1** and **2** may be caused by the large and flat 2, 2'-bipyridyl ligand.

The coordination sphere of complex **3** is similar to that of complex **2**, but the manganese ion of the complex **3** has a more distorted octahedral environment with N_2O_4 donor set consisted by two nitrogen atoms from phenathroline, three oxygen atoms from mefenamic acid and one oxygen atom from methanol. Two mefenamic acid ligands are different, one is monodentate, while the other one is bidentate. That may lead to the more distorted coordination environment of manganese centre in the complex **3** comparing to the complexes **1-2**. The different coordination modes of two mef ligands in complex **3** also result in the different Mn-O bond distances. The oxygen atom of monodentate mef (Mn(1)-O(1), 2.100(2) Å) is closer to the manganese centre than the oxygen atoms of bidentate mef (Mn(1)-O(1′), 2.267(2); Mn(1)-O(2′), 2.220(2)). As shown in Table 2, the angel of N(2)-Mn-N(2′) is well agreed with the similar structure reported before.[27] Because of the large phenathroline ligand, the overall structure of the complex **3** is as bulky as the complex **2**, both are much larger than the complex **1**.

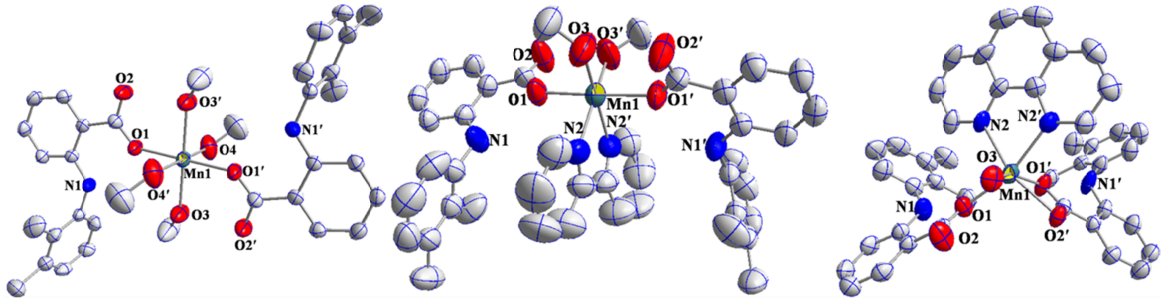

Complex 1 **Complex 2** **Complex 3**

Fig. 1 Crystal structures of the complexes **1-3.**

Table 1 Crystallographic Data for the Complexes **1-3**.

Parameter	1	2	3
Empirical formula	$C_{36}H_{52}MnN_2O_{10}$	$C_{42}H_{44}MnN_4O_6$	$C_{42}H_{38}MnN_4O_5$
Formula weight	727.74	755.75	733.70
Crystal system	Triclinic	Orthorhombic	Triclinic
Space group	*P*-1	*Iba*2	*P*-1
a(Å)	7.733(15)	7.425(4)	9.584(4)
b(Å)	8.013(16)	29.560(2)	12.224(5)
c(Å)	15.932(3)	17.582(14)	15.873(7)
α(◦)	91.59(3)	90	96.746(7)
β(◦)	95.39(3)	90	96.434(8)
γ(◦)	92.27(3)	90	97.868(8)
Volume(Å^3)	981.5(3)	3859.1(5)	1806.8(13)
Z	1	4	2
Reflections collected	7049/4310[*R*(int)= 0.0569]	8896/4167[*R*(int)= 0.0466]	9150/6323[*R*(int) =0.0455]
Data/restrains/parameters	4310 / 0 / 228	4167 / 8 / 243	6323 / 0 / 479
GOF on F^2	0.965	0.875	1.024
Final R indices[$I>2\sigma(I)$]	R_1 = 0.0703, wR_2 = 0.1639	R_1 = 0.0493, wR_2 = 0.913	R_1 = 0.0534, wR_2 = 0.691
R indices (all data)	R_1 = 0.1243, wR_2 = 0.1868	R_1 = 0.1188, wR_2 = 0.1045	R_1 = 0.1360, wR_2 = 0.789
CCDC no	931669	931670	955463

Spectroscopic characterizations

The FT-IR spectra of the all three complexes show two typical broad bands in the ranges of 1609-1613 cm^{-1} and 1385-1391 cm^{-1} due to asymmetric and symmetric C=O vibrations of the mef ligand, respectively. The IR vibrations are summarized in Table S1. The peak at 3300 cm^{-1} was assigned as N-H vibration, and the peak at 3440 cm^{-1} was O-H vibration. The stretching modes of three complexes are almost identical, indicating that the coordination of the ligand to the manganese centre is in a similar mode, which is consistent with the elemental analysis and crystal structures. Although in the complex **3**, one of the mef is bidentate ligand, IR spectra cannot resolve that.

The UV-visible spectra of the complexes **1-3** in borate buffer were also recorded as shown in Fig. 2. The bands at 287, and 340 nm in all three complexes were ascribed to the π-π* transition of the mef ligand. In complex **3**, band at 265 nm is contributed by the ligand phen. All three complexes do not show absorbance in the visible region (400-800 nm), which is the case for many Mn(II) complexes.[27]

The state of the three complexes in solution was also investigated by electronspray ionization mass spectrometry (ESI-MS), because they are critical for their LOX-1 inhibitory activity. A peak at m/e 568.2 ($[Mn(mef)_2(CH_3OH)H]^+$) corresponding to the loss of three methanol molecules in complex **1** was observed. Similarly, the monocations $[Mn(mef)_2(bipy)H]^+$(m/e 692.9) and $[Mn(mef)(phen)(DMF)]^+$ (m/e 548.1) were observed in complexes **2** and **3**, respectively. The results indicate that the ligand mef is coordinated to manganese ions even in solution, however, it is possible they are in hydrolyzed forms, which can not be determined by the current data.

Lipoxygenase inhibitory activity

The functional mechanism of mef is generally believed through inhibition to LOX and/or COX.[28-29] LOX-1 inhibitory activity of the three complexes was thus examined with linoleic acid as a substrate. The *cis*, *cis*-1,4-pentadiene of linoleic acid can be easily oxidized by LOX-1 to form *cis*, *trans*-hydroperoxydiene derivative, which shows maximum absorption at 235 nm, thus can be used as a spectral handle to monitor the LOX-1 activity.[29] The contribution from the complexes at 235 nm was removed by subtracting the spectra of the complexes alone under the same condition. As shown in Fig. 3, $MnCl_2$ shows no LOX-1 inhibitory activity, while mef and the three Mn-mef complexes show obvious inhibitory activity. IC_{50} of the mef and the complexes **1-3** are 78.67, 16.79, 38.63, and 28.06 μM, respectively. Among them, complex **1** showed much higher inhibitory activity than the others. For instance, more than 80% activity of LOX-1 was inhibited by 100 μM of the complex **1**, and over 60% and 70% activity of LOX-1 was inhibited under the same concentration by the complexes **2** and **3**, respectively. While for the ligand mef, only about 50% of the activity of LOX-1 was inhibited, suggesting that the Mn-mef complexes are more effective LOX-1 inhibitors than that of the parent ligand mef. The higher inhibitory activity of the Mn-mef complex could be caused by high concentration of mef, because each Mn-mef complex contains two mef ligands. To exclude this possibility, the state of the Mn-mef complexes in solution was measured by MS spectrometry. It is found that the mef ligand is in coordinated state in solution.

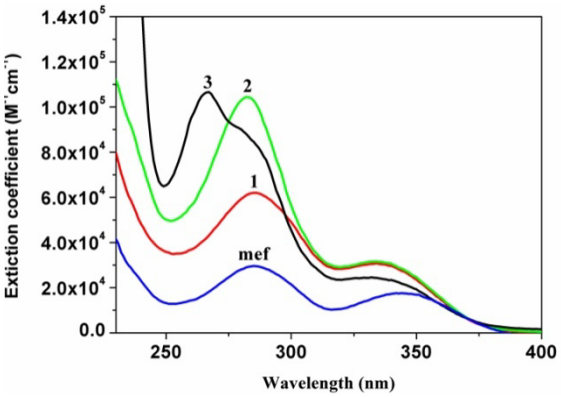

Fig. 2 UV-visible spectra of the complexes **1-3** and ligand mefenamic acid in H_3BO_3-NaOH buffer (0.1 M, pH 9.0). The complexes were first dissolved into methanol (complexes **1** and **2**) or DMF (complex **3**), then take 10 μL of the concentrated solution and dispersed into 1 mL of the buffer.

Table 2. Selected Bond Distances (Å) and Angles (deg) for Compounds **1**−**3**.

1		2		3	
Mn(1)-O(1)	2.129(19)	Mn(1)-O(1)	2.126(2)	Mn(1)-O(1)	2.100(2)
Mn(1)-O(1′)	2.129 (19)	Mn(1)-O(1′)	2.126(2)	Mn(1)-O(1′)	2.267(2)
Mn(1)-O(3)	2.202(2)	Mn(1)-O(3)	2.141(4)	Mn(1)-O(2′)	2.220 (2)
Mn(1)-O(4)	2.213(3)	Mn(1)-O(3′)	2.141(4)	Mn(1)-O(3)	2.159(3)
Mn(1)-O(4′)	2.213(3)	Mn(1)-N(2)	2.232(4)	Mn(1)-N(2)	2.270(3)
Mn(1)-O(3′)	2.202(2)	Mn(1)-N(2′)	2.232(4)	Mn(1)-N(2′)	2.262(3)
O(1)-Mn(1)-O(1′)	180.00	O(1)-Mn(1)-O(1′)	177.4(2)	O(1)-Mn(1)-O(1′)	96.79(9)
O(1)-Mn(1)-O(3)	92.35(8)	O(1′)-Mn(1)-O(3′)	92.13(13)	O(1)-Mn(1)-O(2′)	103.00(8)
O(1)-Mn(1)-O(3′)	87.65(8)	O(1)-Mn(1)-O(3′)	86.14(12)	O(1)-Mn(1)-O(3)	89.15(10)
O(1)-Mn(1)-O(4)	88.69(9)	O(1′)-Mn(1)-O(3)	86.15(12)	O(1)-Mn(1)-N(2)	90.94(10)
O(1)-Mn(1)-O(4′)	91.31(9)	O(1)-Mn(1)-O(3)	92.12(13)	O(1)-Mn(1)-N(2′)	162.97(9)
O(1′)-Mn(1)-O(3)	87.65(8)	O(3′)-Mn(1)-O(3)	96.8(3)	O(3)-Mn(1)-N(2)	104.97(10)
O(1′)-Mn(1)-O(3′)	92.35(8)	O(1′)-Mn(1)-N(3′)	88.18(13)	O(3)-Mn(1)-N(2′)	89.11(11)
O(1′)-Mn(1)-O(4)	91.31(9)	O(1)-Mn(1)-N(3')	93.92(14)	N(2)-Mn(1)-N(2′)	73.17(10)
O(1′)-Mn(1)-O(4′)	88.69(9)	O(3′)-Mn(1)-N(2′)	95.72(17)	O(1′)-Mn(1)-O(2′)	58.22(8)
O(3)-Mn(1)-O(4)	89.42(10)	O(3)-Mn(1)-N(2′)	166.45(17)	O(1′)-Mn(1)-O(3)	156.79(9)
O(3)-Mn(1)-O(4′)	90.58(10)	O(1′)-Mn(1)-N(2)	93.91(14)	O(1′)-Mn(1)-N(2)	97.37(9)
O(3′)-Mn(1)-O(4)	90.58(10)	O(1)-Mn(1)-N(2)	88.19(13)	O(1′)-Mn(1)-N(2′)	91.42(10)
O(3′)-Mn(1)-O(4′)	89.42(10)	O(3′)-Mn(1)-N(2)	166.44(17)	O(2′)-Mn(1)-O(3)	98.59(9)
O(3)-Mn(1)-O(3′)	180.00	O(3)-Mn(1)-N(2)	95.72(17)	O(2′)-Mn(1)-N(2)	152.77(9)
O(4)-Mn(1)-O(4′)	180.00	N(2′)-Mn(1)-N(2)	72.4(2)	O(2′)-Mn(1)-N(2′)	94.01(9)

To understand the inhibition mechanism of the Mn-mef complexes, the kinetics of the LOX-1 was investigated in the absence or presence of the Mn-mef complexes. It is found that K_m of the LOX-1 is increased, while V_{max} remains the same in the presence of complex **1** and mef; while K_m remains the same as that of the native enzyme in the presence of complexes **2** and **3** based on the Line weaver–Bulk plots (Fig. S1). The values of K_m, V_{max}, K_{cat} and K_i in the presence of three Mn-mef complexes were summarized in Table 3. Similar kinetics data was observed when (Z)-9-palmitoleyl sulfate inhibited LOX-1.[30] These results indicate that the complex **1** and mef are competitive inhibitors, while complexes **2** and **3** are non-competitive inhibitors. K_i values of the complexes **1-3** and mef also revealed that the order of inhibitory activity is **1**>>**2**, **3**, and mef. The highest inhibitory

activity and competitive inhibitory mode of the complex **1** suggest that it may interact with LOX-1 in a unique mode.

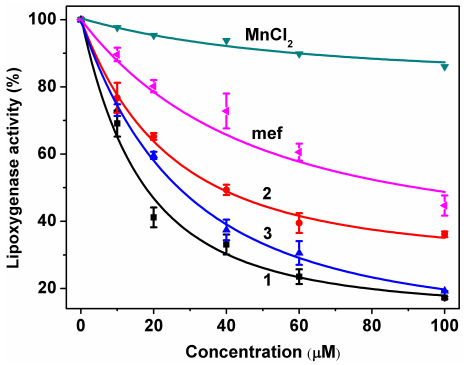

Fig. 3 Comparison of the LOX-1 inhibitory activities of the complexes **1-3**, $MnCl_2$, and mefenamic acid. Reaction condition: linoleic acid (0.75 mM), LOX-1 (1×10^{-6} mM) in H_3BO_3-NaOH buffer (0.1 M, pH 9.0) at 20 ℃.

Table 3. Kinetic Parameters of LOX-1 Oxidizing Linoleic Acid in the Absence and Presence of the Complexes **1-3** and Mef.

	V_{max}(Ms^{-1})	K_m(M)	K_{cat}(s^{-1})	K_{cat}/K_m($M^{-1}s^{-1}$)	K_i(M)
-	2.35×10^{-7}	1.67×10^{-5}	2.35×10^{2}	1.40×10^{7}	0
1	2.35×10^{-7}	3.72×10^{-5}	2.35×10^{2}	6.41×10^{6}	1.08×10^{-3}
2	1.23×10^{-7}	1.67×10^{-5}	1.23×10^{2}	7.36×10^{6}	7.52×10^{-4}
3	1.07×10^{-7}	1.67×10^{-5}	1.07×10^{2}	6.41×10^{6}	3.01×10^{-4}
mef	2.35×10^{-7}	2.61×10^{-5}	2.35×10^{2}	9.00×10^{6}	2.71×10^{-4}

Computer Docking

To identify the binding mode of the three Mn-mef complexes to LOX-1, computer docking was carried out. The binding site of natural substrate fatty acid to LOX-1 has been much debated.[31-33] On the basis of crystal structure of LOX-1, Boyington *et al.* suggested a narrow passage with sharp bends near the Fe atom and the constriction formed by the side chains is one of possible

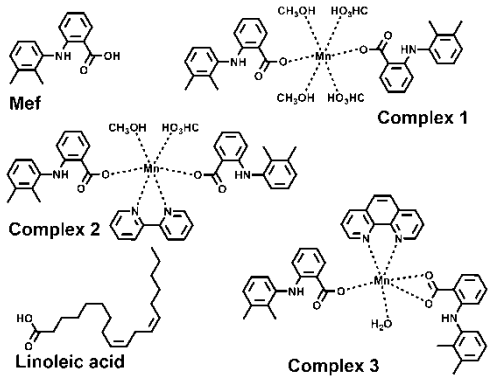

Fig. 4 Chemical structures of three Mn-mef complexes and its ligand mef, substrate linoleic acid of LOX-1 that used in the docking.

binding cavities for the fatty acid substrate (named as cavity II, as displayed in Fig. S2).[34] Similarly, the portion of the cavity II that is close to the Fe (named as cavity II_a) was believed as a probable binding site.[35] However, the cavity II is wholly internal, and the substrate has to first enter the sub-cavity II_b after a rearrangement of the side chains, then pass a convoluted path as much as 40 Å in length to reach the cavity II_a. The long path and high energy necessary to replace all water molecules in the path made this proposal not realistic.[35] One promising alternative substrate binding site is at the opposite end of cavity II_a, far away from cavity II_b and relatively close to the Fe atom (shown in Fig. S2b) based on a higher resolution of the crystal structure of LOX.[23] In this case, the access to the cavity II_a is only barred 8-10 Å from the Fe atom by a gate composed with three residues from two chains (Thr259, Lys260 and Leu541). This substrate binding site is believed more likely, because the adjustment of the gate is not only sterically unhindered, but also is sufficient to open a wide channel for entry of a fatty acid.[23] We, therefore docked substrate linoleic acid, mef and the complexes **1-3** with LOX-1 at the area that centring at the atom Fe and covering the cavities II_a and II_b (radius of ~ 25 Å, volume ~6.5×10^4 $Å^3$, Fig. S2a) using Molegro Virtual Docker program (MVD). The chemical structures of the linoleic acid, mef, and the complexes **1-3** are shown in Fig. 4. The best results showed that linoleic acid could be docked inside the cavity II_a, and is close to the Fe centre with a distance of 6 Å from its pentadiene moiety (C9-13) to Fe atom as shown in Fig. 5a (yellow molecule). The orientation of the linoleic acid is agreed with the result reported by Gardner *et al*, it bends inside the cavity II_a with its tail in the vicinity of the gate (Thr259, Leu260 and Lys541) and polar head is in the pocket.[23]

The complex **1** was docked in the cavity II_a (Fig. 5b, red molecule) similar to the substrate linoleic acid. One mef ligand in complex **1** takes the same orientation as the linoleic acid. It interacted with Ile751 and Gln495 residues of LOX-1 through hydrogen bonding as shown in Fig. 6a (indicated by blue lines). It also interacted with other residues at the cavity II_a of LOX-1 *via* weak interactions, such as Thr259, His504, and His499. Among them, Thr259 is one of the residue that composing the gate to the cavity II_a, the other two residues are the ligands of Fe centre. The similarity of the docked position of linoleic acid and the complex **1** indicates that the complex **1** entered the cavity II_a through the gate like linoleic acid. Thus the binding of complex **1** to LOX-1 is able to block the access of the linoleic acid to the active site, which is consistent with the competitive inhibitory activity of the complex **1** observed in the experiment. Interestedly, when mef was docked with LOX-1, the best docking result is that mef located inside the cavity II_a (blue molecule in Fig. 5c), but is different from the linoleic acid, and overlapped with one mef lignad of the complex **1** (Fig. 5d). Therefore, the inhibition by mef to LOX-1 is competitive but the inhibitory activity is lower than that of the complex **1**, which is consistent with the experimental result (Table 3).

In contrast, the complexes **2** and **3** cannot be docked inside the cavity II_a as the complex **1** does. Instead, they can be best docked at the position with ~ 3 Å away from the cavity II_a (Fig. 5d, black and orange molecules outside the cavity II_a). The complex **2** interacts with LOX-1 mainly through hydrogen bonds with Tyr493, Asp578, Asp584, Lys587, Gln579, and Asn502 residues (Fig. 6b), and the complex **3** is mainly stabilized by three hydrogen bonds with Tyr493, Val570 and Asn573 (Fig. 6c).

It is possible other weak interactions between the complex **2** and the residues of LOX-1 also contribute to their interactions. The interaction with these residues may affect the activity of the LOX-1, because they are adjacent to the ligands of Fe atom. Therefore, complex **2** exerts its effect on LOX-1 catalytic activity through affecting the conformation of the active site of LOX-1, which eventually induces the non-competitive inhibition to

linoleic acid oxidation as observed experimentally. Similarly, the complex **3** also interacts weakly with other residues as shown in Fig. 6c. However, these residues only indirectly interact with the residues that are critical to the activity of LOX-1, therefore inhibitory activity of the complexes **2** and **3** are much lower than the complex **1**. However, the interactions with the residues need to be further confirmed by the site-directed mutagenesis of LOX-1.

The difference in the binding of the complexes **1** and **2**, **3** to LOX-1 originated from their structural differences. As shown in Fig. 1, two ligands extend from two sides of the octahedral manganese centre in the complex **1**, while the two mef ligands in the complex **2** are oriented in same direction of the two sides of the Mn-bipy plane, and they are even more expanded in the complex **3**. Thus the bulky complexes **2** and **3** cannot enter the cavity II_a as easy as the complex **1**. Actually, if taking a closer look at the environment of the complex **1** docked inside cavity II_a, one can see that the complex **1** was surround closely by the residues Gln495, Leu546, Ile553, and Leu754 (Fig. S2b), complexes **2** and **3** are definitely too large to be fitted in this room.

Combining the aforementioned docking and experimental results, we conclude that the inhibitory activity of the Mn-mef complexes **1-3** to LOX-1 is determined by their binding mode to LOX-1, which is in turn decided by their spatial arrangements. To further confirm this result, we also synthesized Co-mef complexes with similar structures, which have been reported exhibiting LOX-1 inhibitory activity too.[15] As expected, three Co-mef complexes showed the same inhibition trend

Fig. 5 The binding modes of linoleic acid, mef, the complexes **1**, **2** and **3**, at the cavity II_a (gray net region) of LOX-**1**. Three residues, Thr259, Lys260 and Leu541 that gate the entrance of the cavity II_a are displayed. The active site of LOX-1, Fe atom along with its coordination ligands (His 499/504/690, Ile839, and Asn694) are also displayed. (a) linoleic acid (yellow), (b) mef (blue), (c) complex **1** (red), and (d) overlay of the (a), (b), and (c); and the complexes **2** (black) and **3** (orange) that docked at the outside of the cavity II_a.

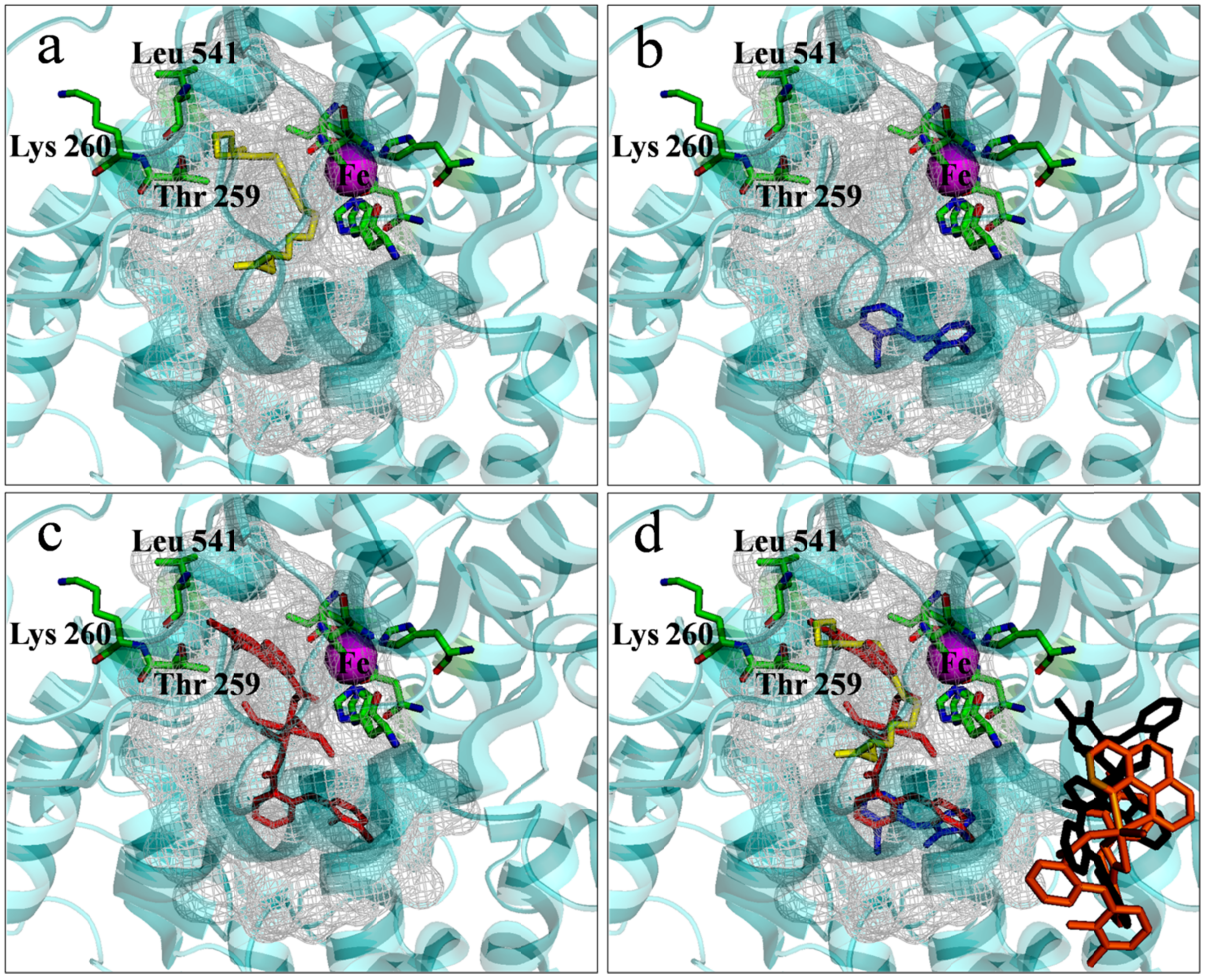

Cite this: DOI: 10.1039/c0xx00000x

www.rsc.org/xxxxxx

ARTICLE TYPE

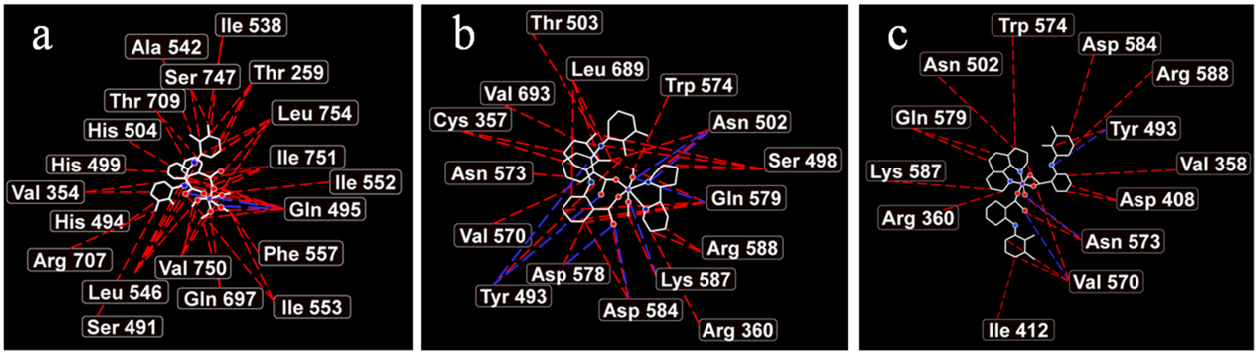

Fig. 6 Ligand maps of the three complexes bind to the LOX-1 (for clarity, hydrogen bonds with waters were excluded, blue dotted lines indicate hydrogen bonds; red dotted lines indicate steric interaction). (a) complex **1**; (b) complex **2**; and (c) complex **3**.

as Mn-mef complexes. $Co(mef)_2(CH_3OH)_4$ exhibited a strong competitive inhibition to LOX-1 as the complex **1** does; while $Co(mef)_2(bipy)(CH_3OH)_2$ and $Co(mef)_2(phen)(CH_3OH)_2$ showed weak non-competitive inhibition as the complexes **2** and **3**, respectively (data not shown). These results corroborated unambiguously that the structures of the metal-mef complexes determine their interaction with the enzyme consequently leading to different enzyme inhibitory activities. To this aspect, the role of metal ion in metal-mef is more structural, the unique geometry of the metal-mef complexes orient the ligand to the right binding site of the enzyme. Variety of metal complexes in addition to Mn-mef and Co-mef are necessary to discover the other roles of metal ions, however, different metal complexes may have different structures, which may complicate the question.

Anti-oxidant Activity of the Complexes 1-3

As reported for many other metal-NSAID complexes, the anti-oxidant activity of NSAIDs that closely related to their anti-inflammatory activity, usually is improved at a certain extent *via* the coordination to metal ions comparing to the parent NSAID ligand.[14] In order to evaluate anti-oxidant activity of the three Mn-mef compounds, the ability of scavenging free radical DPPH is measured. DPPH with a strong absorption at 517 nm in methanol becomes colourless when accepting an electron,[36] thus the absorption change at 517 nm of DPPH in the presence of the Mn-mef complexes can be used to measure the radical scavenging activity of the complexes. There is a fast decrease phase after adding the complexes **1-3** to DPPH solution in the first ~ 3 min, then a gradual change is observed (Fig. S3). The contribution of manganese ions alone was negligible under this condition. Three complexes showed a similar trend. Under the different complex concentrations, we found that the free radical scavenging abilities of three complexes are in order: **2**>>**3** and **1**, while ligand mef and $MnCl_2$ barely exhibit any activity as shown in Fig. 7. This data is comparable to the copper complex, however, it was reported that dinuclear $Cu_2(mef)_4(H_2O)_2$ was much better than the mononuclear complexes.[16] The radical

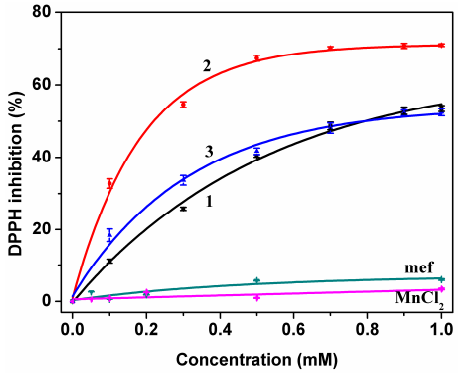

Fig. 7 Radical scavenging rates *versus* different concentrations of the complexes **1-3**, mef, and $MnCl_2$ in methanol for 30 min. DPPH is 30 μM.

scavenging activity by the complexes **1-3** was also confirmed by EPR measurements. All three complexes showed a similar behaviour as shown in Fig. S4 using complex **2** as an example. The EPR signal of DPPH is quenched drastically in the first 3 minutes after the addition of the complex indicating the strong radical scavenging activity of the complex.

The anti-oxidant activity of the complexes was also characterized complementarily through inhibiting SOD activity. For comparison, the activity of ligand mef and $MnCl_2$ were measured under the same conditions. Complexes **1-3** exhibit SOD activity inhibition of 65.73%, 82.00%, and 70.14% at a concentration of 0.5 μM, respectively (Fig. S5). While the ligand mef and $MnCl_2$ exhibit very low activity. Declan *et al.* reported Mn-monensin complexes under the same experimental condition showed SOD inhibitory activity of 67.5%, respectively.[37] The complexes **2** and **3** are again slightly active than the complex **1**, which is consistent with the radical scavenge results.

Conclusions

Three Mn-mef complexes were synthesized and characterized with UV-visible, IR, elemental analysis, and X-ray crystal

diffraction. The pharmaceutical performances of the three complexes were explored in parallel with the parent ligand mef. We found that the Mn-mef complexes displayed higher LOX-1 inhibitory activity than that of the ligand mefenamic acid. The inhibitory activity of the complexes is closely related to their spatial arrangements, which decide their interaction modes with the LOX-1. Complex **1** that contains two mef ligands inhibits the enzyme activity competitively, while the bulky and low symmetry complexes **2-3** tend to inhibit the enzyme activity uncompetitively. The computer docking of the three complexes and ligand mef with the LOX-1 is highly consistent with the experimental results. The smaller size metal complexes and ligand itself are likely to bind competitively at the substrate binding site, while the bulky complexes cannot enter the substrate binding site, and thus inhibit the enzyme activity uncompetitively *via* binding to the enzyme at different sites. The anti-oxidant activity of the Mn-mef complexes is also improved comparing to the parent drug, which is apparently originated from the metal centre. The coordination of mef to manganese ions improves the anti-inflammatory activity of mef either by enhancing its LOX-1 inhibitory activity, and/or increasing their anti-oxidant ability *via* manganese centre. We demonstrated that metal-NSAID complexes are better anti-inflammatory drug candidates than NSAIDs, because they have unique structures that could interact with the target enzymes more specifically. In addition, metal ions introduce extra anti-oxidant activity to metal-NSAID complexes.

Supporting information

The Line weaver-Burk plot for the inhibition of LOX-1 by complex **1-3**; the docking area in this work, and the spatial environment of the complex 1docked inside the cavity II_a of LOX-1; DPPH radical scavenging by the complexes **1-3**; SOD inhibitory activity, and the selected IR data for the complexes **1-3** are supplied as Supporting Information.

Acknowledgements

This research was carried out with financial support from the National Science foundation of China (Nos. 21001044 and 31070742), the state key laboratory of bioreactor engineering (No. 2060204), 111 Project (No. B07023), and the Shanghai Committee of Science and Technology (No. 11DZ2260600).

References

1. C. P. Duffy, C. J. Elliott, R. A. O'Connor, M. M. Heenan, S. Coyle, I. M. Cleary, K. Kavanagh, S. Verhaegen, C. M. O'Loughlin, R. NicAmhlaoibh, M. Clynes, *Eur. J. Cancer,* 1998, **34**, 1250–1259.
2. F. Catella-Lawson, M. P. Reilly, S. C. Kapoor, A. J. Cucchiara, S. Demarco, B. Tournier, S. N. Vyas, G. A. Fitzgrerald, *N. Engl. J. Med.,* 2001, **345**, 1809-1817.
3. J. R. Vane, Regina M Botting, *Am. J. Med.,* 1998, **104**, 2S-8S.
4. L. A. G. Rodriguez, *Clin. Exp. Rheumatol. ,* 2001, **19**, S41-S44.
5. I. Bjamason, J. Hayllar, A. J. MacPherson, A. S. Ressell, *Gastroenterology,* 1993, **104**, 1832-1847.
6. P. Amadio, D. M. Cummings, P. Amadio, *Postgrad Med.,* 1993, **93**, 73–97.
7. N. Ouyang, P. Ji, J. L. Williams, *Int. J. Oncol.,* 2012, **42**, 643-650.
8. M. Elkady, R. Nieß, A. M. Schaible, J. Bauer, S. Luderer, G. Ambrosi, O. Werz, S. A. Laufer, *J. Med. Chem.,* 2012, **55**, 8958-8962.
9. J. E. Weder, C. T. Dillon, T. W. Hambley, B. J. Kennedy, P. A. Lay, J. R. Biffin, H. L. Regtop, N. M. Davies, *Coord. Chem. Rev.,* 2002, **232**, 95-126.
10. C. T. Dillon, T. W. Hambley, B. J. Kennedy, P. A. Lay, Q. D. Zhou, N. M. Davies, J. R. Biffin, H. L. Regtop, *Chem. Res. Toxicol.,* 2003, **16**, 28-37.
11. M. Konstandinidou, A. Kourounakis, M. Yiangou, L. Hadjipetrou, D. Kovala-Demertzi, S. Hadjikakou, M. Demertzis, *J. Inorg. Biochem.,* 1998, **70**, 63-69.
12. A. S. Fernandes, J. Gaspar, M. F. Cabral, C. Caneriras, R. Guedes, J. Rueff, M. Castro, J. Costa, N. G. Oliverira, *J. Inorg. Biochem.,* 2007, **101**, 849-858.
13. C. V. Winder, J. Wax, L. Scotti, R. A. Scherrer, E. M. Jones, F. W. Short, *J. Pharmacol. Exp. Ther.,* 1962, **138**, 405-413.
14. D. Kovala-Demertzi, D. Hadjipavlou-Litina, M. Staninska, A. Primikiri, C. Kotoglou, M. A. Demertzis, *J. Enzyme Inhib. Med. Chem.,* 2009, **24**, 742-752.
15. F. Dimiza, A. N. Papadopoulos, V. Tangoulis, V. Psycharis, C. P. Raptopoulou, D. P. Kessissoglou, G. Psomas, *Dalton Trans.,* 2010, **39**, 4517-4528.
16. F. Dimiza, S. Fountoulaki, N. P. Athanasios, C. A. Kontogiorgis, V. Tangoulis, C. P. Raptopoulou, V. Psycharis, A. Terzis, D. P. Kessissoglou, G. Psomas, *Dalton Trans.,* 2011, **40**, 8555-8568.
17. V. Dokorou, A. Primikiri, D. Kovala-Demertzi, *J. Inorg. Biochem.,* 2011, **105**, 195-201.
18. B. P. Skowronska, R. Kaczorowska, T. Skowronski, *Environ. Pollut.,* 1997, **97**, 65-69.
19. D. Hamai, S. C. Bondy, *Neuoochem Int*. 2004, **44**, 223-229.
20. E. J. Underwood, Academic press, New York, Fourth ed., 1997.
21 B. K. Wagnont, S. C. Jackels, *Inorg. Chem.,* 1988, **28**, 1923-1927.
22. B. Axelrod, T. M., C. S. Laakso, *Methods Enzymol.,* 1981, **71**, 441-451.
23. W. Minor, J. Steczko, B. Steczko, Z. Otwinowski, J. T. Bolin, R. Walter, B. Axelrod, *Biochemistry,* 1996, **35**, 10687-10701.
24. R. Thomsen, M. H. Christensen, *J. Med. Chem.,* 2006, **49**, 3315-3321.
25. E. Vrontaki, G. Leonis, M. G. Papadopoulos, M. Simcic, S. G. Grdadolnik, A. Afantitis, G. Melagraki, S. K. Hadjikakou, T. Mavromoustakos, *J. Chem. Inf. Model.,* 2012, **52**, 3293-3301.
26. M. Saldias, V. Paredes-Garcia, A. Vega, W. Cañon Mancisidor, F. E. Le, D. V. Yazigi, E. Spodine, *Polyhedron,* 2012, **41**, 120-126.
27. X. J. Jiang, H. Liu, B. Zheng, J. Y. Zhang, *Dalton Trans.,* 2009, **0**, 8714-8723.
28. R. G. Kurumbail, A. M. Stevens, J. K. Gierse, J. J. McDonald, R. A. Stegeman, J. Y. Pak, D. Gildehaus, J. M. Iyashir, T. D. Penning, K. Seibert, P. C. Isakson, W. C. Stallings, *Nature,* 1996, **384**, 644-648.
29. S. Fiorucci, R. Meli, M. Bucci, G. Cirino, *Biochem. Pharmacol.,* 2001, **62**, 1433-1438.
30. V. C. Ruddat, S. Whitman, T. R. Holman, C. F. Bernasconi, *Biochemistry,* 2003, **42**, 4172-4178.
31. H. W. Gardner, *Biochim. Biophys. Acta,* 1989, **1001**, 274-281.
32. J. M. LaLonde, D. A. Bernlohr, L. J. Banaszak, *Biochemistry* 1994, **33**, 4885-4895.
33. A. C. M. Young, G. Scapin, A. Kromminga, S. B. Patel, J. H. Veerkamp, J. C. Sacchettini, *Structure,* 1994, **2**, 523-534.
34. J. C. Boyington, B. J. Gaffney, L. M. Amzel, *Science,* 1993, **260**, 1482-1486.
35. M. L. Connolly, *Science,* 1983, **221**, 709-713.
36. M. S. Blois, *Nature,* 1958, **181**, 1199-1200.
37. A. E. O. Fisher, G. Lau, D. P. Naughton, *Biochem. Biophys. Res. Commun.,* 2005, **329**, 930-933.